

Enrichment of two isomeric heparin oligosaccharides exhibiting different affinities towards MCP-1

*Rebecca L. Miller^{1,3}, *Andrew B. Dykstra^{1,4}, Wei Wei¹, Cynthia Holsclaw¹, Jeremy E. Turnbull², Julie A. Leary¹.

¹Departments of Molecular and Cellular Biology and Chemistry, University of California, 1 Shields Dr. Davis, CA 95616 USA.

²Centre for Glycobiology, Department of Biochemistry, Institute of Integrative Biology, University of Liverpool, Crown Street, Liverpool, L69 7ZB, England, UK;

³Current address: Department of Oncology, University of Oxford, Old Road Campus, Oxford, OX3 7DQ

⁴Current address: Attribute Sciences, Process Development, Amgen, Thousand Oaks, CA

Corresponding authors:

Rebecca L. Miller, University of California and University of Oxford

Email address: rebecca.miller@oncology.ox.ac.uk

Prof. Julie A. Leary

Email address: jleary@ucdavis.edu

*Joint first authors

Abstract

Chemokine-GAG interactions are crucial to facilitate chemokine immobilization, resulting in the formation of chemokine gradients that guide cell migration. Here we demonstrate chromatographic isolation and purification of two heparin hexasaccharide isomers that interact with the oligomeric chemokine MCP-1/CCL2 with different binding affinities. The sequences of

these two hexasaccharides were deduced from unique MS/MS product ions and HPLC compositional analysis. IM-MS (Ion mobility mass spectrometry) showed that the two isolated oligosaccharides have different conformations and both displayed preferential binding for one of the two distinct conformations known for MCP-1 dimers. A significant shift in arrival time distribution of close to 70 \AA^2 was observed, indicating a more compact protein:hexasaccharide conformation. Clear differences in the MS spectra between bound and unbound protein allowed calculation of K_d values from the resulting data. The structural difference between the two hexasaccharides was defined as the differential location of a single sulfate at either C-6 of glucosamine or C-2 of uronic acid in the reducing disaccharide, resulting in a 200 fold difference in binding affinity for MCP-1. These data indicate sequence specificity for high affinity binding, supporting the view that sulfate position and not simply the number of sulfates, is important for HS-protein binding.

Introduction

Heparin and heparan sulfate (HS) are part of the GAG family of linear polysaccharides, composed of a repeating disaccharide building block of a uronic acid (glucuronic acid or its epimer, iduronic acid, which can be sulfated at the carbon 2 position), and glucosamine (which can be O-sulfated on the carbon 6 and rarely, carbon 3 position, while the N-group can contain either a sulfate, an acetate, or a free amine)⁵. Variability in the extent and patterns of sulfation gives rise to a high diversity of structures and functions⁶.

Highly basic patches on chemokine proteins make them likely binding partners both *in vitro* and *in vivo*⁷⁻⁹, and chemokine–GAG interactions are thought to facilitate chemokine

immobilization, resulting in the formation of a directed chemokine gradient to guide cell migration and prevent dissociation under the shear forces of blood flow^{1, 7, 10}. Under these conditions, the GAGs provide an anchor, protection against proteolysis, and a site-specific concentration gradient¹¹⁻¹³. Mutagenesis of putative GAG-binding sites on chemokines shows the functional relevance of this interaction¹⁴⁻¹⁵.

Chemokine oligomerization is thought to be a hallmark of chemokine function, with very few chemokines functioning as monomers *in vivo*. The formation of chemokine oligomers has also been strongly associated with chemokine–GAG interactions¹⁶⁻¹⁹. For MCP-1/CCL2 GAG binds to both dimer and tetramer states^{14, 20-21}. Mutations in the key binding residues (Arg¹⁸, Lys¹⁹, Arg²⁴, and Lys⁴⁹) causes decreased ability to bind heparin and form complexes. Interestingly, the mutation P8A-CCL2 prevents oligomerization, and although heparin was still able to bind *in vitro*, *in vivo* leukocyte adhesion and migration were not observed^{14, 22-23}. This was unexpected as GAG binding results in oligomerization and both are a requirement for *in vivo* receptor activation and it would be expected that both processes would be affected *in vivo*^{14, 22-23}. Interestingly, chemokines with this mutation are linked with a significant reduction in adjuvant-induced arthritis²²⁻²³. While most studies have focused on the mutation of the MCP-1/CCL2 protein, structural changes in HS during disease progression may also play a role²⁴. Indeed, it has been observed that HS structures change depending on the severity of rheumatoid arthritis²⁴. Other protein–GAG disease progression models have also shown structural changes to the GAG chain²⁵⁻²⁶. Nevertheless, sequence-specific interactions have only been identified in a handful of cases; for MCP-1/CCL2 O-sulfation is possibly more relevant than N-sulfation²⁷ and there is a preference towards highly sulfated regions²⁸⁻³⁰.

Interestingly, MCP-1 is predominantly upregulated in rheumatoid arthritis³¹, resulting in upregulation of cytokines and an inflammatory response that causes the enzymatic digestion of connective tissues. Small anionic molecules, nucleotides and peptides have shown promise for inhibiting protein-GAG oligomerization³²⁻³⁵, but it is logical to use GAGs³⁶ as these molecules are known regulators of MCP-1 activation and inhibition^{14, 34, 37-39}. However, due to the complexity observed within GAGs, the isolation of single saccharide species is challenging. Separation methods for heparin and HS oligosaccharides have improved over the last 10 years, with new chromatography methods using graphite⁴⁰⁻⁴¹, hydrophilic interaction chromatography (HILIC)⁴² and cetyltrimethylammonium strong anion exchange (CTA-SAX)⁴³. Recently we described a novel CTA-SAX method using volatile salts (Miller *et al*, submitted to *Analytical Chemistry*) which together with other established HPLC techniques now offers enhanced capabilities for high purity separations of heparin / HS oligosaccharides. We rationalized that it might now be possible to purify smaller MCP-1 binding saccharides, since this would be preferable to gain greater target specificity and fewer undesirable side effects, as shown with the anticoagulant pentasaccharide drug, Arixtra⁴⁴.

Herein, we used tandem SAX separations and affinity chromatography in combination with ion mobility and tandem MS to show that MCP-1 does show a preference towards highly sulfated regions, although a high amount of negative charge alone was insufficient for increased binding affinity. Two highly sulfated isomeric structures displayed drastically different affinities towards MCP-1. This indicates that sequence and conformation of the GAG are both important for binding, and that the isolation of purified isomeric structures is required to properly elucidate protein-GAG interactions and their functional consequences.

Experimental methods

Materials and reagents

All chemical and biochemical products were of analytical grade and purchased from VWR (Lutterworth, UK) and Sigma (Gillingham, UK) unless otherwise indicated. Disaccharide standards 1–8 were purchased from V-Laboratories (Covington, LA) except for standard 3, which was obtained from Iduron (Manchester, UK). Heparin was purchased from Alfa Aesar (Massachusetts, USA). All materials were digested with recombinant heparinase enzymes I, II and III obtained from IBEX (Canada).

Digestion of heparin

Heparin (1 g) was reconstituted in 500 μ L of lyase buffer (100 mM sodium acetate, 10 mM calcium acetate). Enzyme reactions were performed using 1 mU of heparinase I to 10 mg of heparin and were incubated at 37 °C. The reaction was stopped at set time points; 2, 3, 4, 6 and 8 hours by removing a 120 μ L aliquot and denaturing heparinase I at 98 °C for 3 minutes. All aliquots were pooled and the resulting products were further separated as described below.

Size exclusion chromatography (SEC)

SEC separations were performed on a Waters Delta 600 HPLC system (Waters Corp., Milford, MA, USA) using a Biorad Econo column packed in-house with preparation grade Superdex 30 beads (15 mm \times 170 cm, bead size 34 μ m – GE Healthcare). A 500 mg sample of pooled digested heparin was made up to a total of 1 mL, injected and separated using an eluent of 0.5 M ammonium bicarbonate at a flow rate of 0.1 mL / minute. The elution profile was monitored with an absorbance at 232 nm. Fractions containing heparin oligosaccharides were

pooled and repeatedly freeze-dried using HPLC grade water until all the ammonium bicarbonate was removed.

C18-strong anion exchange chromatography (SAX)

MCP-1 (25 nM) and a heparin dp6 (25 nM) SEC fraction were incubated for 30 minutes in a 0.1 M NaCl solution with a total volume of 50 μ L. This reaction was then loaded at 10 μ L / minute onto a C18 trap BDS silica column (15 mm \times 2.1 mm, 5 μ m bead size – Sigma). The flow-through was cycled around the C18 column three times to ensure complete loading⁴⁵. Equilibration of the column was completed using a Delta 600 HPLC (Waters) in eluent A for 20 minutes at 0.2 mL / minute to ensure that all the unbound oligosaccharide had been eluted from the column. The C18 trap column was coupled with a Propac PA1 column (4.6 mm \times 250 mm, 5 μ m bead size – Dionex) and equilibrated in eluent A for 20 minutes at 0.2 mL / minute. C18-SAX separations were performed using a Delta 600 HPLC (Waters), with a UV-visible spectrophotometric detector. The elution profiles were monitored with an absorbance at 232 nm. A linear gradient of 0.1 M–1.4 M NaCl was generated appropriately by mixing eluents A and B over 90 minutes, using a flow rate of 0.2 mL / minute for the elution, at a temperature of 40 °C. Appropriate fractions were desalted in HPLC grade water using a Hitrap desalting column (GE Healthcare) on an isocratic path.

Strong anion-exchange chromatography (SAX)

Separation of SEC fractions were performed on a Waters Delta 600 HPLC system (Waters Corp., Milford, MA, USA) using a SAX Propac PA1 column (4.6 mm \times 250 mm, 5 μ m bead size – Dionex). Eluent A was HPLC-grade water and eluent B was 2 M NaCl. A dp6 SEC fraction was injected and loaded on to the column, and a gradient of 0 M–1.4 M NaCl was

generated appropriately by mixing eluents A and B over 90 minutes using a flow rate of 1 mL / minute for the elution, at a temperature of 40 °C. Subsequent shallower SAX gradients were generated using the same instrument, column and eluents, with the gradient being changed to 0.84 M–1.2 M NaCl over 60 minutes.

VSCTA-SAX chromatography

VSCTA-SAX separations were performed on a Delta 600 HPLC (Waters) using a cetyltrimethylammonium derivatized C18 column (4.6 mm × 250 mm, 5 µm bead size – Sigma) (Miller *et al*, submitted to *Analytical Chemistry*). The C18 column was derivatized with 1 mM cetyltrimethylammonium in water: methanol ratio of 40 : 60 (v/v). Eluent A was HPLC grade water and eluent B was 2 M ammonium bicarbonate. The elution profiles were monitored with an absorbance at 232 nm. Oligosaccharides collected from the Propac PA1 column were diluted 1 in 10 in water and multiple injections were performed to load the sample onto the VSCTA-SAX column. VSCTA-SAX was used to separate peak C further on a 0.8 M – 1.5 M ammonium bicarbonate gradient over 60 minutes using a flow rate of 1 mL / minute, at a temperature of 40 °C. Each fraction was dried on a SPD121B speed vac (Thermo Scientific) prior to mass spectrometry and compositional analysis.

Compositional analysis

Oligosaccharides collected from the VSCTA-SAX column were digested using 10 µL of 1 mU / 1µL, heparinase I, heparinase II and heparinase III to create disaccharides^{46,47-48,49}. The reaction was incubated at 30 °C for 24 hours so that complete digestion could be achieved. Both hexasaccharide structures were digested to disaccharides and separated using a Propac PA1 column on a 0-1 M NaCl gradient over 60 minutes. Disaccharide standards were injected onto

the same column and separated under the same conditions so that the disaccharide standards and the hexasaccharide samples could be compared. Elution profiles were monitored with an absorbance of 232 nm.

IM-MS of isomeric hexasaccharides

IMMS was performed on two purified hexasaccharides using a Synapt G1 mass spectrometer equipped with a T-wave mobility cell (Waters). The Synapt G1 instrument was calibrated in negative ion mode using sodium iodide as a standard. The concentration of each hexasaccharide was calculated based on its absorbance at 232 nm. An 0.5 μ M hexasaccharide concentration in water / acetonitrile (50/50 v/v) with 500 mM ammonium hydroxide was loaded into borosilicate electrospray tips made in-house as previously described⁵⁰. Each hexasaccharide was infused into the mass spectrometer and ionized in negative ion mode using a capillary voltage of 0.55 kV, a sample cone voltage of 7 V and an extraction cone voltage of 0.6 V. The ion mobility parameters were optimized and conditions were identical for each hexasaccharide sample, and all parameters can be found in supplementary materials. MS/MS was performed on m/z of 549.3 $[M-3H]^{3-}$ and collisional activated at 15 V in the transfer cell with the ion mobility cell turned off in order to produce comparable CID (Collision induced dissociation) data for each isomer.

Ion mobility of MCP-1: hexasaccharide complexes

IM-MS of MCP-1: hexasaccharide complex was performed on a Synapt G2 mass spectrometer equipped with a T-wave mobility cell. The hexasaccharide concentrations were calculated based on its 232 nm absorbance and the MCP-1 concentration was based on the expressed, isolated and purified MCP-1 previously described⁵¹. The borosilicate tips were made

in house as stated in previous publications⁵⁰. The Synapt G2 instrument was calibrated with cesium iodide (50 μg / μL) over a mass range of 500 – 8,000. IM-MS data were calibrated as previously described⁵² using the drift times of the 11+ through 21+ charge states of 10 μM horse heart myoglobin in 50 % acetonitrile, 0.1 % formic acid. Data were analysed using Mass Lynx 4.1. MCP-1 was sprayed at a concentration of 10 μM , whereas the hexasaccharides were incubated with MCP-1 at concentrations of 40 μM , 20 μM , 10 μM , 5 μM , and 2.5 μM . Each MCP-1: hexasaccharide sample was sprayed in a borosilcate gold coated tip and each mass spectra were acquired in positive mode with a capillary voltage of 0.78 kV and a sample cone voltage of 17 V. The ion mobility parameters that the instruments were operated in were; trap collision energy, 3 V; transfer collision energy, 0 V; trap DC bias, 40 V; trap gas flow, 4 mL / minute (Ar); IM-MS gas flow, 90 mL / minute (N_2). The backing pressure on the Synapt G2 was optimised to preserve the MCP-1: hexasaccharide complex and was set to 6.5 mBar by regulating the backing scroll pump with a speedi valve. IM-MS wave velocity was set to 725 m/s and the IM-MS wave height was set to 40 V. A 32 kV radio frequency generator was used to supply voltage to the quadrupole. LM resolution was set to 4.7 and HM resolution was set to 15.

Results and Discussion

C18 affinity enrichment method for MCP-1: oligosaccharide interactors

Heparin oligosaccharides were digested by heparinase I and separated using SEC chromatography (Supporting Information, Figure S-1) to obtain size defined fractions. Each fraction was collected and then analyzed using mass spectrometry to determine the dominant size of oligosaccharides within each SEC peak (data not shown). A dp6 (hexasaccharide) mixture was chosen, as this is likely to contain both MCP-1 activators and inhibitors with strong specificity.

Hexasaccharides that bind to MCP-1 were then isolated using a two dimensional C18-SAX affinity method (Figure 1). The hexasaccharide mixture was first passed through the two dimensional column in the absence of MCP-1 to identify the elution positions of all hexasaccharides in the mixture (Figure 1a). MCP-1 was then incubated with the hexasaccharide mixture before the MCP-1-hexasaccharide complexes were bound to the C18 column. Hexasaccharides that formed MCP-1 complexes and which were amenable to dissociation with salt, were captured and resolved using a Propac SAX column (Figure 1b). Peak A was present in trace (a) but reduced in trace (b), indicating that both MCP-1 binding and nonbinding saccharides were present in the peak. As peak A elutes at higher salt concentrations, it is likely to have a higher number of sulfate groups and thus it was chosen, as a candidate, to probe the various isomeric structures and their affinities for MCP-1.

Other affinity methods have been used to identify differential binding to heparin / HS, including biotinylated proteins⁵³, so we also performed this enrichment method as a comparison. The major drawback to this method is that biotinylated MCP-1 binds to streptavidin in a monomeric state, not the naturally occurring dimer (Figure S-2). The streptavidin bound MCP-1: hexasaccharide complex only retained the final oligosaccharide peak, unlike the C18 bound MCP-1: hexasaccharide complex. Protein: oligosaccharide assembly dynamics are the likely reason for this result. Subunit packing and conformational changes are critical for biological affinity, and these would be more naturally observed with the C18-SAX method.

Preparative scale purification of MCP-1 binders and non-binders

To further purify isomeric hexasaccharides from Peak A and obtain sufficient material for characterization, preparative scale dp6 oligosaccharide separation (Figure S-1) and C18-SAX oligosaccharide separation were repeated under the same conditions as shown in Figure 1. Peak

A was identified in the preparative oligosaccharide SAX separation based on elution position and was further purified (Figure 2a). Peak A was separated using a shallower SAX gradient (Figure 2b), resulting in the separation of two subsequent peaks, peak B and peak C (Figure 2b). Peak C was separated by VSCTA-SAX chromatography into two further peaks (Figure 2c), peak D and peak E. Although baseline resolution was not observed between peaks D and E, both were successfully collected and shown to be pure compounds. The lack of baseline resolution is not uncommon in the separation of heparin oligosaccharides^{49, 54}, thus the partial collection of each peak is required to isolate pure structures.

Ion mobility and sequencing of two isomeric structures

To confirm that peak D and peak E were indeed different structures, IM-MS was performed on both (Figure 3a). Arrival time distributions (ATD) of peak D exhibited a more compact structural conformation with an ATD of 3.46 ms, whereas peak E exhibited a more extended conformation with an ATD of 3.60 ms (Figure 3a). MS of compounds D and E showed that both structures had the same molecular ion at m/z of 549.3 $[M-3H]^{3-}$ (data not shown). Oligosaccharides with this m/z correspond to a $dp6 + 8SO_3$. Tandem mass spectrometry of hexasaccharide D and hexasaccharide E resulted in different product ion spectra (Figure 3b, Figure S-3 and Figure S-4), which is not unusual for MS/MS of GAG isomers⁵⁵. As expected, the product ions for both spectra showed sulfation losses and a doubly-charged product ion at m/z of 576, corresponding to $dp4 + 6SO_3$. As $dp4 + 6SO_3$ is fully sulfated, both hexasaccharide D and E contain two repeating tri-sulfated disaccharides, but differ in the sulfation of the third disaccharide unit (Figure S-3 and S-4). Compositional analysis⁴⁷ confirmed that both hexasaccharides contained $\Delta U A 2 S - G l c N S 6 S$, while hexasaccharide D contained $\Delta U A - G l c N S 6 S$ and hexasaccharide E contained a $\Delta U A 2 S - G l c N S$ (Figure 3c). This leaves the

possibility of two structural sequences for hexasaccharide D Δ UA2S - GlcNS6S - UA2S - GlcNS6S - UA - GlcNS6S and Δ UA - GlcNS6S - UA2S - GlcNS6S - UA2S - GlcNS6S and for hexasaccharide E Δ UA2S - GlcNS6S - UA2S - GlcNS6S - UA2S - GlcNS and Δ UA2S - GlcNS - UA2S - GlcNS6S - UA2S - GlcNS6S. Analysis of the B, Y, C and Z ions allowed determination of the sequence from unique cross ring cleavages (Figure S-3 and S-4). MS/MS confirmed that the structure of hexasaccharide D is Δ UA2S - GlcNS6S - UA2S - GlcNS6S - UA - GlcNS6S, and the structure of hexasaccharide E is Δ UA2S - GlcNS6S - UA2S - GlcNS6S - UA2S - GlcNS.

MCP-1: hexasaccharide interactions

Under IM-MS conditions, MCP-1 exists in two conformations as a homodimer. One is the α conformation, which is more compact while the other is the β conformation, which exhibits a more extended conformation resulting from the flexible N-terminal region within MCP-1²⁰. As a control, MCP-1 (in the absence of any hexasaccharide) was sprayed under native conditions and the MCP-1 dimer at m/z, 2171 was extracted from the IM-MS chromatogram. ATD for the two conformations are shown in Figure 4a. To ensure that no other MCP-1 assembly was present at the same m/z as the MCP-1 dimer: hexasaccharide complex (which would appear at m/z 2377), this ion was also extracted from the IM-MS chromatogram (Figure 4b). Figure 4b clearly shows an absence of any conflicting or overlapping ATD at the m/z of 2377.

To further identify binding of the purified hexasaccharides, IM-MS was performed on MCP-1 dimer complexes with hexasaccharides D and E, respectively (Figures 4c - 4f). Incubation of hexasaccharide D with MCP-1 (Figure 4c and 4d) produced the same α and β conformations of the MCP-1 dimer but the ATD showed very different relative intensities for the two conformers, with the β form being only 29% of the level of the α form (Table S-1). Data in

Figure 4d indicates that hexasaccharide D preferred to complex with only one conformation of the MCP-1 dimer (β) as evidenced by the single peak in Figure 4d and the clear depletion in abundance of the β conformation in Figure 4c and Table S-1. The MCP-1 dimer: hexasaccharide D complex resulted in a collisional cross section (CCS) (1804 \AA^2) indicative of further folding to a more compact structure compared to the unbound beta MCP-1 dimer with a CCS of 1875 \AA^2 . ATD shown in Figures 4e and 4f also indicated a preference for the β - conformer complex upon binding of hexasaccharide E, albeit to a much less degree than hexasaccharide D (Table S-1). This may be due to the flexible N-terminal regions that bridge across the protein upon oligosaccharide binding²⁰, as it is known that this region of MCP-1 induces oligomerization with GAG binding and anchoring of the N-terminal region into a more fixed position^{14, 21, 56}. Site directed mutations of single, double and triple knockouts of positivity charged residues validated this heparin interaction⁵⁶. A mutation in the N-terminal region P8A-MCP-1 prevented oligomerization upon interaction with heparin and affected MCP-1 ability to induce *in vivo* leukocyte adhesion and migration²²⁻²³. The flexible N-terminal region is required for oligomerization and previous data showed that MCP-1: GAG interaction caused a conformational change; thus it would be expected that the same conformation change is being observed in the ATD upon MCP-1: GAG binding of hexasaccharide D and E.

To better address the observed differences between the two conformations, the K_d for each interaction was calculated using the following equation:

$$K_d = [\text{free MCP-1}][\text{free hexasaccharide}] / [\text{bound MCP-1 hexasaccharide complex}]$$

Since the intensities of free protein, free hexasaccharide and bound protein–hexasaccharide are known from the MS spectra (Figure S-5), it is possible to calculate a K_d value by altering only the hexasaccharide concentration¹⁷. The K_d value calculated from MS spectra of the MCP-1 dimer: hexasaccharide D complex displayed strong association kinetics (Figure 5 and Figure S-5), and resulted in a relatively strong value of 1.12 μM . A K_d value for hexasaccharide E cannot be ascertained with certainty due to the weak interaction with MCP-1, showing a quadratic curve as linear, resulting in a large error associated with this value. What can be shown from the data is that hexasaccharide E is a relatively weak binder of MCP-1 compared to hexasaccharide D (Figure 5). It is unlikely that hexasaccharide E would have been retained in the affinity enrichment method as competitive stoichiometry would have bound a higher affinity structure.

Crystallography has identified MCP-1 as existing in both dimer and tetramer complexes upon GAG interaction^{20, 57}; however, although tetrameric complexes are believed to exist, biological evidence to date only supports MCP-1 dimerization. ATD of the tetramer complex isolated from the IM-MS chromatogram is shown in Figure S-6. MCP-1 in the absence of a hexasaccharide (Figure S-6a and b), showed that MCP-1 had a CCS of 2041 \AA^2 . The MCP-1 tetrameric complex with and without hexasaccharide D (Figure S-6c and d) showed no change in the ATD, whereas the ratio of free tetrameric MCP-1 to hexasaccharide D bound tetrameric MCP-1 was ~ 4 -fold larger. MCP-1 tetrameric complex with and without hexasaccharide E (Figure S-6e and f) again showed no change in the ATD, whereas the ratio of free tetrameric MCP-1 to hexasaccharide D bound tetrameric MCP-1 was decreased ~ 5 -fold.

Conclusions

In this study we used a C18-SAX affinity methodology to identify specific isomeric oligosaccharides that bind differentially to MCP-1.

Both hexasaccharides D and E meet the known binding requirements for MCP-1 (i.e. they are highly sulfated with eight negative charges), however, one structure bound with high affinity and the other with significantly lower affinity. The sulfation difference between the two structures is the position of a sulfate on C-6 of glucosamine and a sulfate on C-2 of the uronic acid. Knowing that MCP-1 prefers highly sulfated structures, it is possible that the sulfate on C-2 might inhibit, and/or the sulfate on the C-6 might promote stronger interactions with MCP-1. This is further complicated by changes in the hexasaccharide conformation due to the position of the O-sulfate, making the molecule physically unfavorable to fit in the protein binding pocket.

Regardless of the exact mechanism, our data does indicate that MCP-1 has significant sequence specificity for heparin/HS, with the sulfate position, not just the number of sulfates, is critical for high affinity binding. Here we demonstrated an approach for purification and identification of specific isomeric structures with different protein binding properties. For MCP-1 we anticipate that this will allow further isolation and purification of specific oligosaccharides that may show different biological activities towards the protein and possibly afford development of new treatments for inflammatory diseases.

References

1. Johnson, Z.; Proudfoot, A. E.; Handel, T. M., *Cytokine Growth Factor Rev* **2005**, *16* (6), 625-36.
2. Rot, A., *Immunol Today* **1992**, *13* (8), 291-4.
3. Salanga, C. L.; Handel, T. M., *Exp Cell Res* **2011**, *317* (5), 590-601.
4. Hardy, L. A.; Booth, T. A.; Lau, E. K.; Handel, T. M.; Ali, S.; Kirby, J. A., *Lab Invest* **2004**, *84* (1), 81-90.
5. Bame, K. J.; Venkatesan, I.; Stelling, H. D.; Tumova, S., *Glycobiology* **2000**, *10* (7), 715-26.
6. Turnbull, J.; Powell, A.; Guimond, S., *Trends Cell Biol* **2001**, *11* (2), 75-82.
7. Hoogewerf, A. J.; Kuschert, G. S.; Proudfoot, A. E.; Borlat, F.; Clark-Lewis, I.; Power, C. A.; Wells, T. N., *Biochemistry* **1997**, *36* (44), 13570-8.
8. Witt, D. P.; Lander, A. D., *Curr Biol* **1994**, *4* (5), 394-400.
9. Kuschert, G. S.; Coulin, F.; Power, C. A.; Proudfoot, A. E.; Hubbard, R. E.; Hoogewerf, A. J.; Wells, T. N., *Biochemistry* **1999**, *38* (39), 12959-68.
10. Handel, T. M.; Johnson, Z.; Crown, S. E.; Lau, E. K.; Proudfoot, A. E., *Annu Rev Biochem* **2005**, *74*, 385-410.
11. Ellyard, J. I.; Simson, L.; Bezos, A.; Johnston, K.; Freeman, C.; Parish, C. R., *J Biol Chem* **2007**, *282* (20), 15238-47.
12. Middleton, J.; Neil, S.; Wintle, J.; Clark-Lewis, I.; Moore, H.; Lam, C.; Auer, M.; Hub, E.; Rot, A., *Cell* **1997**, *91* (3), 385-95.
13. Middleton, J.; Patterson, A. M.; Gardner, L.; Schmutz, C.; Ashton, B. A., *Blood* **2002**, *100* (12), 3853-60.

14. Lau, E. K.; Paavola, C. D.; Johnson, Z.; Gaudry, J. P.; Geretti, E.; Borlat, F.; Kungl, A. J.; Proudfoot, A. E.; Handel, T. M., *J Biol Chem* **2004**, *279* (21), 22294-305.
15. Proudfoot, A. E.; Fritchley, S.; Borlat, F.; Shaw, J. P.; Vilbois, F.; Zwahlen, C.; Trkola, A.; Marchant, D.; Clapham, P. R.; Wells, T. N., *J Biol Chem* **2001**, *276* (14), 10620-6.
16. Proudfoot, A. E.; Handel, T. M.; Johnson, Z.; Lau, E. K.; LiWang, P.; Clark-Lewis, I.; Borlat, F.; Wells, T. N.; Kosco-Vilbois, M. H., *Proc Natl Acad Sci U S A* **2003**, *100* (4), 1885-90.
17. Dykstra, A. B.; Sweeney, M. D.; Leary, J. A., *Biomolecules* **2013**, *3* (4), 905-22.
18. Rueda, P.; Balabanian, K.; Lagane, B.; Staropoli, I.; Chow, K.; Levoye, A.; Laguri, C.; Sadir, R.; Delaunay, T.; Izquierdo, E.; Pablos, J. L.; Lendinez, E.; Caruz, A.; Franco, D.; Baleux, F.; Lortat-Jacob, H.; Arenzana-Seisdedos, F., *PLoS One* **2008**, *3* (7), e2543.
19. Laguri, C.; Sadir, R.; Rueda, P.; Baleux, F.; Gans, P.; Arenzana-Seisdedos, F.; Lortat-Jacob, H., *PLoS One* **2007**, *2* (10), e1110.
20. Seo, Y.; Andaya, A.; Bleiholder, C.; Leary, J. A., *J Am Chem Soc* **2013**, *135* (11), 4325-32.
21. Crown, S. E.; Yu, Y.; Sweeney, M. D.; Leary, J. A.; Handel, T. M., *J Biol Chem* **2006**, *281* (35), 25438-46.
22. Shahrara, S.; Proudfoot, A. E.; Park, C. C.; Volin, M. V.; Haines, G. K.; Woods, J. M.; Aikens, C. H.; Handel, T. M.; Pope, R. M., *J Immunol* **2008**, *180* (5), 3447-56.
23. Handel, T. M.; Johnson, Z.; Rodrigues, D. H.; Dos Santos, A. C.; Cirillo, R.; Muzio, V.; Riva, S.; Mack, M.; Deruaz, M.; Borlat, F.; Vitte, P. A.; Wells, T. N.; Teixeira, M. M.; Proudfoot, A. E., *J Leukoc Biol* **2008**, *84* (4), 1101-8.
24. Sabol, J. K.; Wei, W.; Lopez-Hoyos, M.; Seo, Y.; Andaya, A.; Leary, J. A., *Matrix Biol* **2014**, *40*, 54-61.

25. Hull, R. L.; Peters, M. J.; Perigo, S. P.; Chan, C. K.; Wight, T. N.; Kinsella, M. G., *J Biol Chem* **2012**, *287* (44), 37154-64.
26. Lawrence, R.; Brown, J. R.; Al-Mafraji, K.; Lamanna, W. C.; Beitel, J. R.; Boons, G. J.; Esko, J. D.; Crawford, B. E., *Nat Chem Biol* **2012**, *8* (2), 197-204.
27. Schenauer, M. R.; Yu, Y.; Sweeney, M. D.; Leary, J. A., *J Biol Chem* **2007**, *282* (35), 25182-8.
28. Yu, Y.; Sweeney, M. D.; Saad, O. M.; Crown, S. E.; Hsu, A. R.; Handel, T. M.; Leary, J. A., *J Biol Chem* **2005**, *280* (37), 32200-8.
29. Sweeney, M. D.; Yu, Y.; Leary, J. A., *J Am Soc Mass Spectrom* **2006**, *17* (8), 1114-9.
30. Meissen, J. K.; Sweeney, M. D.; Girardi, M.; Lawrence, R.; Esko, J. D.; Leary, J. A., *J Am Soc Mass Spectrom* **2009**, *20* (4), 652-7.
31. Furie, M. B.; Randolph, G. J., *Am J Pathol* **1995**, *146* (6), 1287-301.
32. Gong, J. H.; Ratkay, L. G.; Waterfield, J. D.; Clark-Lewis, I., *J Exp Med* **1997**, *186* (1), 131-7.
33. Kulkarni, O.; Pawar, R. D.; Purschke, W.; Eulberg, D.; Selve, N.; Buchner, K.; Ninichuk, V.; Segerer, S.; Vielhauer, V.; Klussmann, S.; Anders, H. J., *J Am Soc Nephrol* **2007**, *18* (8), 2350-8.
34. Arefieva, T. I.; Krasnikova, T. L.; Potekhina, A. V.; Ruleva, N. U.; Nikitin, P. I.; Ksenevich, T. I.; Gorshkov, B. G.; Sidorova, M. V.; Bespalova Zh, D.; Kukhtina, N. B.; Provatorov, S. I.; Noeva, E. A.; Chazov, E. I., *Inflamm Res* **2011**, *60* (10), 955-64.
35. Yu, Y.; Sweeney, M. D.; Saad, O. M.; Leary, J. A., *J Am Soc Mass Spectrom* **2006**, *17* (4), 524-35.
36. Casu, B.; Naggi, A.; Torri, G., *Matrix Biol* **2010**, *29* (6), 442-52.

37. Mellor, P.; Harvey, J. R.; Murphy, K. J.; Pye, D.; O'Boyle, G.; Lennard, T. W.; Kirby, J. A.; Ali, S., *Br J Cancer* **2007**, *97* (6), 761-8.
38. Lundin, L.; Larsson, H.; Kreuger, J.; Kanda, S.; Lindahl, U.; Salmivirta, M.; Claesson-Welsh, L., *J Biol Chem* **2000**, *275* (32), 24653-60.
39. Jayson, G. C.; Gallagher, J. T., *Br J Cancer* **1997**, *75* (1), 9-16.
40. Karlsson, N. G.; Schulz, B. L.; Packer, N. H.; Whitelock, J. M., *J Chromatogr B Analyt Technol Biomed Life Sci* **2005**, *824* (1-2), 139-47.
41. Estrella, R. P.; Whitelock, J. M.; Packer, N. H.; Karlsson, N. G., *Anal Chem* **2007**, *79* (10), 3597-606.
42. Staples, G. O.; Bowman, M. J.; Costello, C. E.; Hitchcock, A. M.; Lau, J. M.; Leymarie, N.; Miller, C.; Naimy, H.; Shi, X.; Zaia, J., *Proteomics* **2009**, *9* (3), 686-95.
43. Mourier, P. A.; Viskov, C., *Anal Biochem* **2004**, *332* (2), 299-313.
44. Olson, S. T.; Swanson, R.; Raub-Segall, E.; Bedsted, T.; Sadri, M.; Petitou, M.; Herault, J. P.; Herbert, J. M.; Bjork, I., *Thromb Haemost* **2004**, *92* (5), 929-39.
45. Naimy, H.; Buczek-Thomas, J. A.; Nugent, M. A.; Leymarie, N.; Zaia, J., *J Biol Chem* **2011**, *286* (22), 19311-9.
46. Saad, O. M.; Leary, J. A., *Anal Chem* **2003**, *75* (13), 2985-95.
47. Saad, O. M.; Leary, J. A., *Anal Chem* **2005**, *77* (18), 5902-11.
48. Saad, O. M.; Ebel, H.; Uchimura, K.; Rosen, S. D.; Bertozzi, C. R.; Leary, J. A., *Glycobiology* **2005**, *15* (8), 818-26.
49. Powell, A. K.; Ahmed, Y. A.; Yates, E. A.; Turnbull, J. E., *Nat Protoc* **2010**, *5* (5), 821-33.

50. Leary, J. A.; Miller, R. L.; Wei, W.; Schworer, R.; Zubkova, O. V.; Tyler, P. C.; Turnbull, J. E., *Eur J Mass Spectrom (Chichester, Eng)* **2015**, *21* (3), 245-54.
51. Schenauer, M. R.; Leary, J. A., *Int J Mass Spectrom* **2009**, *287* (1-3), 70-76.
52. Thalassinou, K.; Grabenauer, M.; Slade, S. E.; Hilton, G. R.; Bowers, M. T.; Scrivens, J. H., *Anal Chem* **2009**, *81* (1), 248-54.
53. Friedl, A.; Chang, Z.; Tierney, A.; Rapraeger, A. C., *Am J Pathol* **1997**, *150* (4), 1443-55.
54. Zaia, J., *Mass Spectrom Rev* **2009**, *28* (2), 254-72.
55. Seo, Y.; Andaya, A.; Leary, J. A., *Anal Chem* **2012**, *84* (5), 2416-23.
56. Severin, I. C.; Gaudry, J. P.; Johnson, Z.; Kungl, A.; Jansma, A.; Gesslbauer, B.; Mulloy, B.; Power, C.; Proudfoot, A. E.; Handel, T., *J Biol Chem* **2010**, *285* (23), 17713-24.
57. Lubkowski, J.; Bujacz, G.; Boque, L.; Domaille, P. J.; Handel, T. M.; Wlodawer, A., *Nat Struct Biol* **1997**, *4* (1), 64-9.
58. Seo, Y.; Schenauer, M. R.; Leary, J. A., *Int J Mass Spectrom* **2011**, *303* (2-3), 191-198.
59. de Paz, J. L.; Moseman, E. A.; Noti, C.; Polito, L.; von Andrian, U. H.; Seeberger, P. H., *ACS Chem Biol* **2007**, *2* (11), 735-44.

Acknowledgements

This research was supported by NIH GM47356-20

Supporting Material Available: Figure S-1. SEC separation of heparinase I digested oligosaccharides produced from heparin Figure S-2. MCP-1: hexasaccharide enrichment using streptavidin affinity method. Figure S-3. MS/MS of hexasaccharide D with a schematic of B, Y,

C and Z ions. Figure S-4. MS/MS of hexasaccharide E with a schematic of B, Y, C and Z ions. Figure S-5. Mass spectra of the MCP-1 dimer and its isomeric hexasaccharide complexes. Figure S-6. IMMS ATD of Tetrameric MCP-1: hexasaccharide complexes. Table S-1. Quantitative table of MCP-1 complexes. Supplementary methods (11 pages). This material is available free of charge via the Internet at <http://pubs.acs.org>.

Figure 1. MCP-1: hexasaccharide enrichment using a C18-SAX method. MCP-1 was incubated with a heparin hexasaccharide mixture, resulting in natural oligomerization. MCP-1 complexes were bound to the C18 column and unbound oligosaccharides were removed from the C18 trap before coupling to a SAX column to improve resolution. MCP-1 dissociated hexasaccharides were then eluted with a gradient of 0.1 M - 1.4 M NaCl over 90 minutes. a) The hexasaccharide mixture in the absence of MCP-1 b) The hexasaccharide mixture in the presence of MCP-1.

Figure 2. Preparative scale hexasaccharide purifications of MCP-1 binders and non-binders. a) Preparative SAX separation of the same hexasaccharide mixture used in the affinity enrichment methodology. Peak A was observed to retain compounds that had a preference to be both binders of MCP-1 and non-binders of MCP-1. b) Peak A was separated further on a more shallow 0.84 M – 1.2 M NaCl SAX gradient over 60 minutes, isolating peak B and peak C. c) VSCTA-SAX was used to separate peak C further on a 0.8 M – 1.5 M ammonium bicarbonate gradient over 60 minutes, isolating peak D and peak E.

Figure 3. Sequencing of two isomeric hexasaccharides that exhibited differences in structural conformation a) Ion mobility separation of peak D showed a more compact structural conformation with an ATD of 3.46 ms, whereas ion mobility separation of peak E

showed a more extended structural conformation with an ATD of 3.60 ms. MS showed that both structures had the same m/z of 549.3 $[M-3H]^{3-}$, which corresponds to a $dp6 + 8SO_3$ b) MS/MS of two $dp6 + 8SO_3$ structures (peak D and peak E). c) Compositional analysis of peak D and peak E. Standards 1 to 5 correspond to 1 - $\Delta U A 2 S - G l c N A c$, 2 - $\Delta U A - G l c N S 6 S$, 3 - $\Delta U A 2 S - G l c N S$, 4 - $\Delta U A 2 S - G l c N A c 6 S$, 5 - $\Delta U A 2 S - G l c N S 6 S$

Figure 4. IMMS ATD of MCP-1: hexasaccharide complexes. a) and b) IM-MS of MCP-1 dimer, c) and d) MCP-1 complexed with the hexasaccharide isolated from peak D, e) and f) MCP-1 complexed with the hexasaccharide isolated from peak E. ATD of ions extracted at m/z 2171 (no saccharide bound) and m/z 2377 (hexasaccharide D or E bound to MCP-1 dimer). See texts for full details.

Figure 5. Calculated K_d for two isomeric hexasaccharides in complex with the MCP-1 dimer. a) Calculated K_d of hexasaccharide D complexed with the MCP-1 dimer. b) Calculated K_d of hexasaccharide E complexed with the MCP-1 dimer.

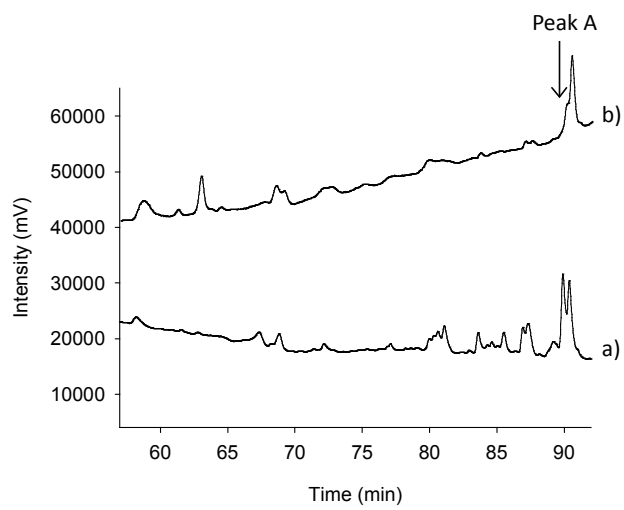


Figure 1. MCP-1: hexasaccharide enrichment using a C18-SAX method.

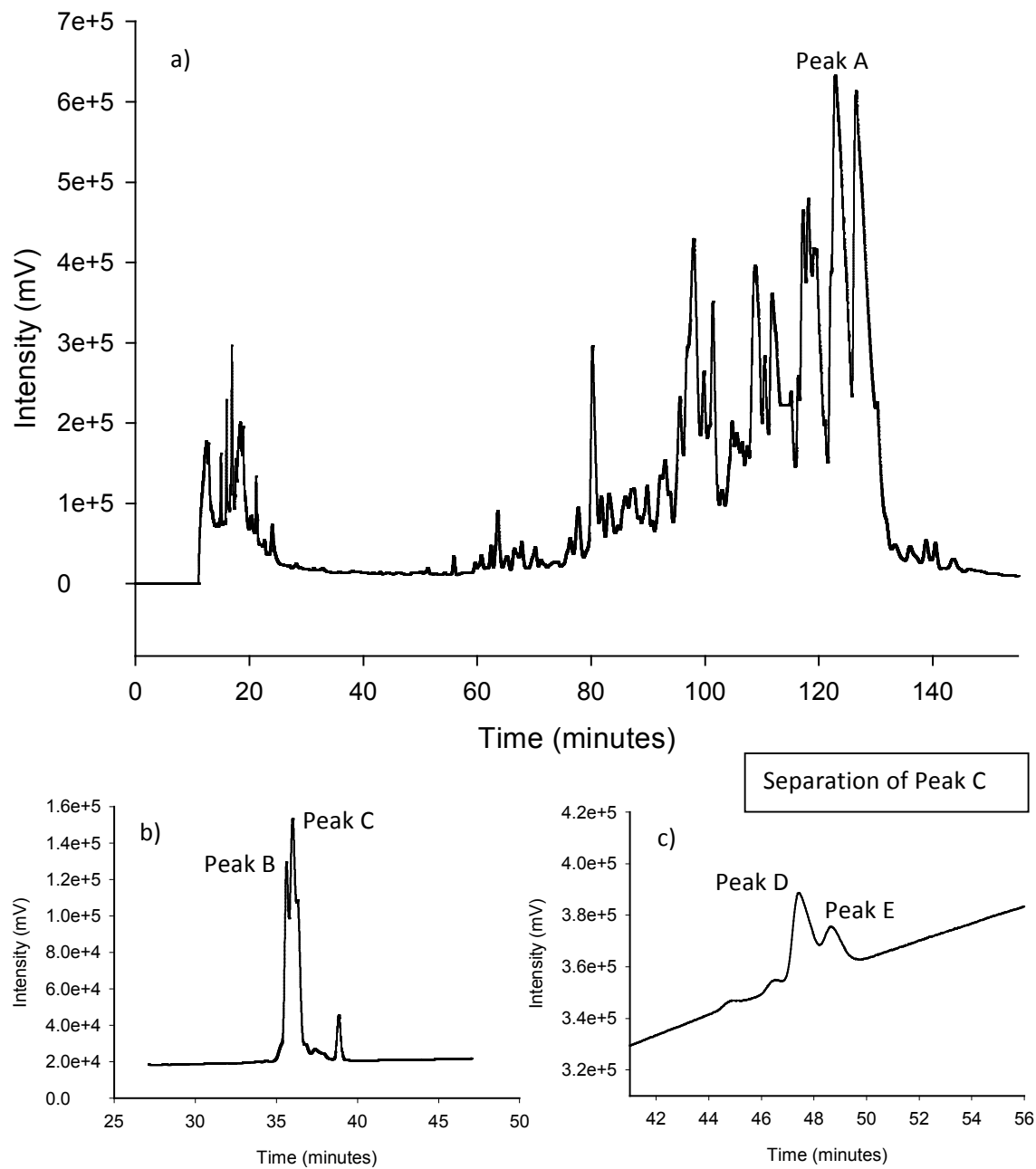


Figure 2. Preparative scale hexasaccharide purifications of MCP-1 binders and non-binders.

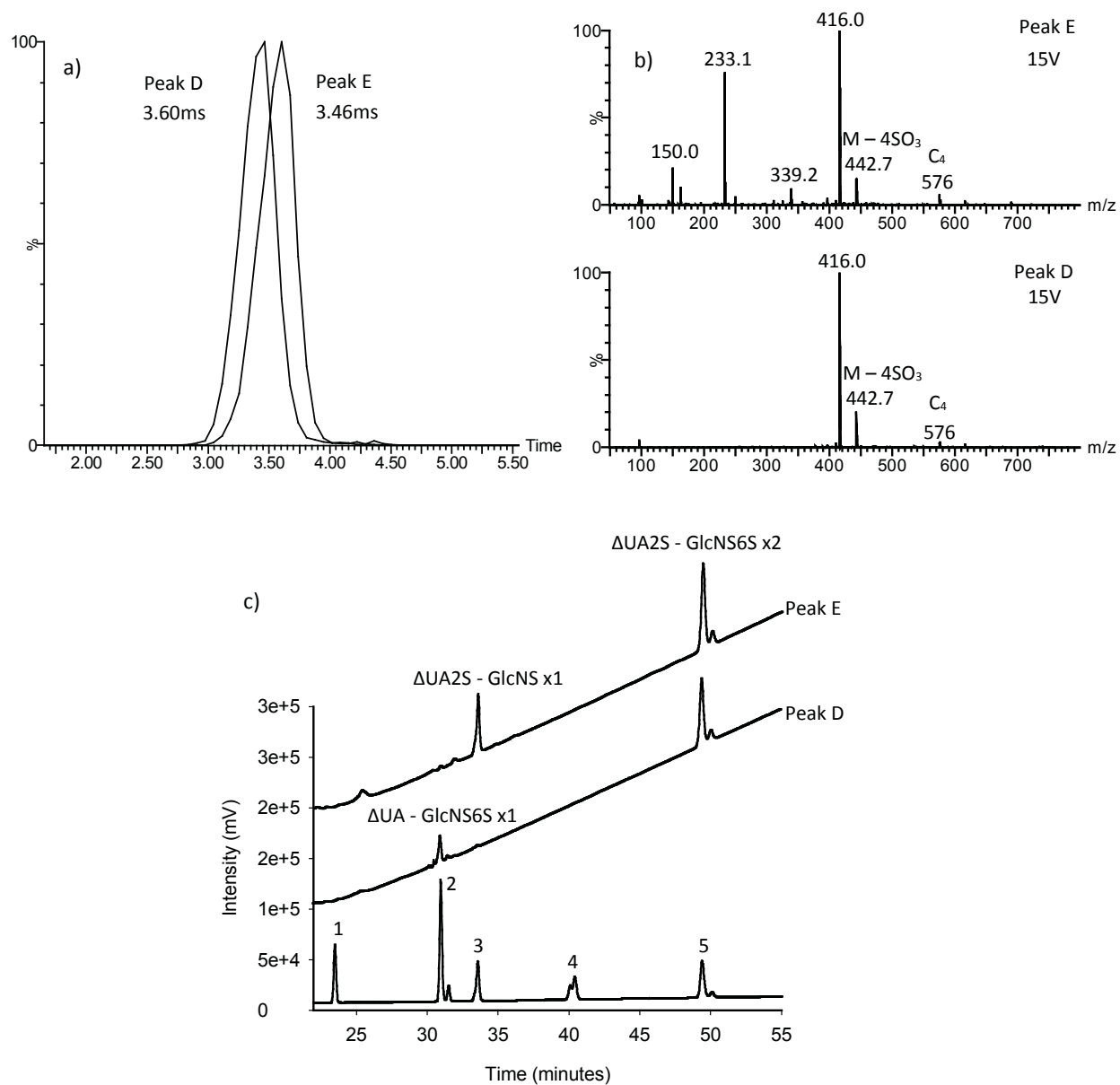


Figure 3. Sequencing of two isomeric hexasaccharides that exhibited differences in structural conformation

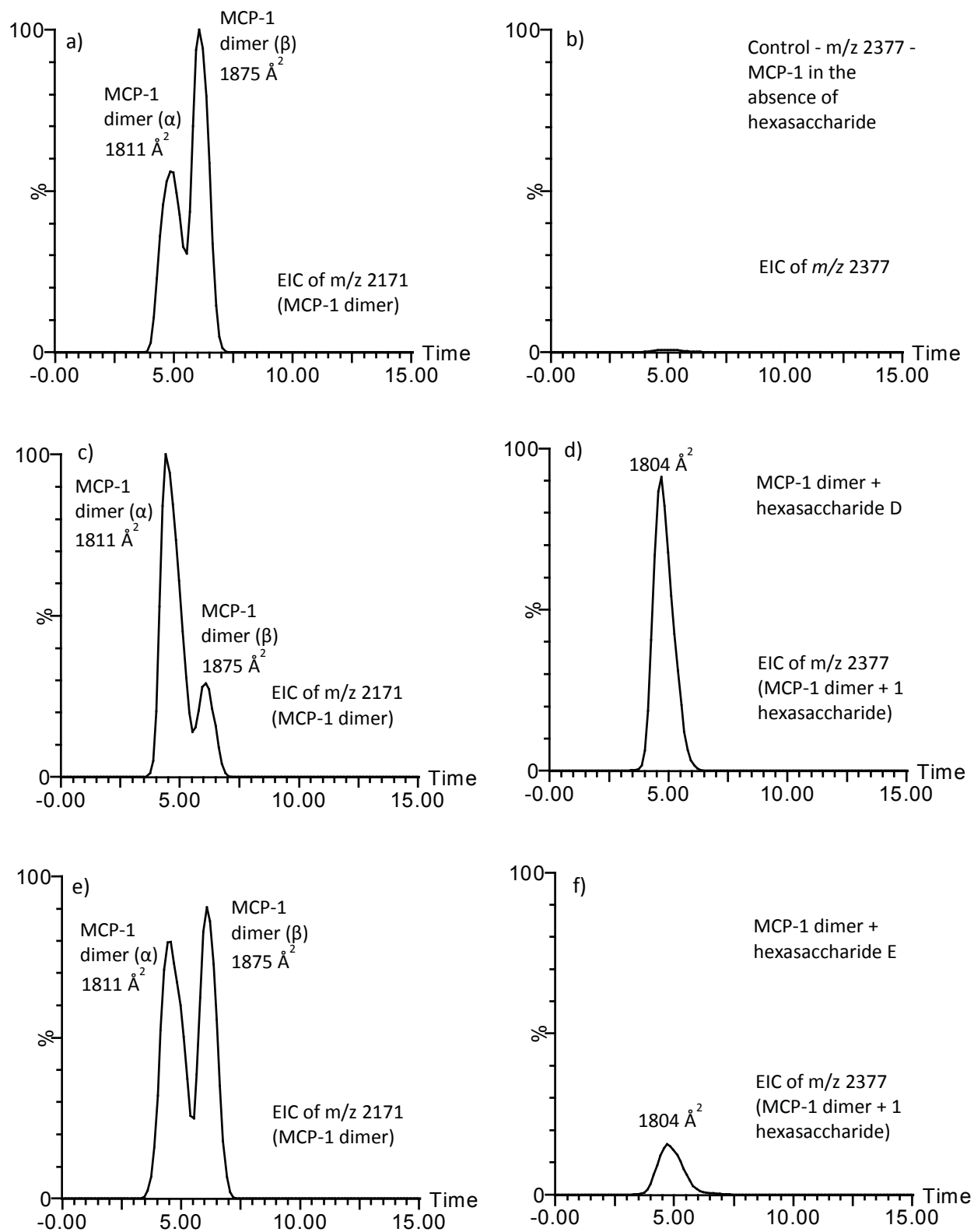
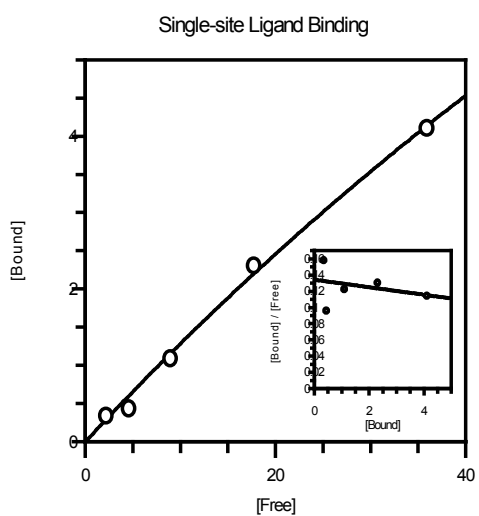
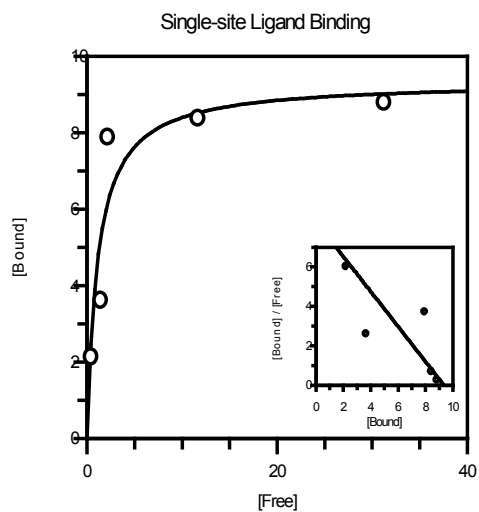


Figure 4. IMMS arrival time distributions (ATD) of MCP-1: hexasaccharide complexes.



	K_d Value	Std Error
Hexasaccharide D	1.1 μM	0.5
Hexasaccharide E	215.8 μM	148.2

Figure 5. Calculated K_d for two isomeric hexasaccharides in complex with the MCP-1 dimer.